Anisotropic performance of a superhydrophobic polyvinyl difluoride membrane with corrugated pattern in direct contact membrane distillation

Yongjie Liu[1,2,3], Jin Wang[1], Zechun Xiao[1,2], Li Liu[1,2,3], Dongdong Li[1], Xuemei Li[1], Huabing Yin[4]*, Tao He[1]*

[1]Shanghai Advanced Research Institute, Chinese Academy of Sciences, Shanghai 201210, China

[2]University of Chinese Academy of Sciences, Beijing 100049, China

[3]School of Physical Science and Technology, ShanghaiTech University, Shanghai 201210, China

[4]School of Engineering, University of Glasgow, Glasgow, G12 8LT, UK

*Corresponding authors: het@sari.ac.cn; huabing.yin@glasgow.ac.uk

Abstract

A novel surface-corrugated superhydrophobic polyvinylidene fluoride (PVDF) membrane (C-PVDF) was prepared for direct contact membrane distillation (DCMD) using a micromolding phase separation (μPS) method. The membrane showed a static contact angle of 159.0 ± 4.0°. However, dynamic measurements of the sliding angles revealed a lower value of 9.1 ± 0.8° when a water droplet slides in parallel to the ridge, and a higher value of 14.6 ± 1.6° if perpendicular to the ridge. This anisotropic property was also reflected in the DCMD fluxes for both feed of deionized water and 4.0 wt.% NaCl solution: in case the feed flows in parallel to the ridge, a higher flux is resulted than it flows perpendicular to the ridge. Anisotropic MD performance cannot be explained by the Dusty-Gas model because the average characteristics of the membrane in the model are intrinsically the same for both flow modes. Instead, anisotropic wetting and sliding in the parallel and perpendicular orientation revealed that the MD performance has both thermodynamic and hydrodynamic origins.

Keywords: superhydrophobic; micromolding phase separation; patterned surface; membrane distillation; anisotropic

1. Introduction

Membrane distillation (MD) is a thermal-driven desalination process utilizing hydrophobic porous membranes [1, 2]. When low grade heat is available, MD can outperform other membrane desalination technologies in terms of high rejection, low capital and operational cost, particularly in treating highly saline liquids [3, 4]. However, limitation in fouling/scaling of hydrophobic membranes has largely constrained the progress of MD in practice.

To solve the fouling/scaling issues in MD membranes, two approaches have normally been exploited: (1) A standard practice via optimization of the process parameters, such as aeration [5], flow rate [6], addition of antiscalants [7], and acidic cleaning of the scaled membrane [8]. (2) Surface engineering for MD membrane from hydrophobic to superhydrophobic or omniphobic. This was pursued as the key solution to improve the fouling and scaling resistance. The development of engineered surface followed the trend from random coating [9], to coating of nanofiber with/without nanoparticles [9-12] to precisely controlled patterned surface [13, 14]. Besides physical modification, the final polishing of the surface is critical as well, mostly by surface deposition or grafting of fluorine-containing chemicals [9, 11, 15-17] or by CF_4 plasma treatment [18-22]. The superhydrophobic or omniphobic properties via combination of physical and chemical modification hold potential to enhance fouling and scaling resistance by mimicking the lotus leave effect [11, 23].

Controlled pattern surface has been recently viewed as a novel platform to understand the fouling/scaling resistance of hydrophobic membrane. Surface patterning of hydrophilic membranes in pressurized filtration has been extensively investigated for microfiltration, ultrafiltration, and reverse osmosis/nanofiltration [24-26]. The resultant increase in the surface

area [27] and shear stress near the membrane surface [24, 28] contribute to increased water flux and improved fouling resistance. A computational fluid dynamics simulation and experimental verification proved that the surface pattern induces high shear stress which decreases the adherence of foulants to the membrane [28, 29].

For hydrophobic membranes, the effect of micropatterns on MD performance has been demonstrated, but far from understood. Membranes with millimeter scale patterns prepared using non-woven spacers showed stable MD flux in processing real seawater and concentrated seawater; extra turbulence created by the corrugated surface structure was attributed to the performance [30]. Nanoimprinted MD membranes with a groove pattern showed a weak hydrophobic interaction with BSA proteins and hence low fouling propensity which was supported by static thermodynamic analysis of adsorption propensity [14]. Recent development of micropillared superhydrophobic membrane showed excellent scaling resistance [4, 13, 31, 32].

To implementing patterned MD membrane in large-scale use, it is highly desirable to develop a cheap flexible mold with large dimension is highly expected. Therefore, we aim to explore a new robust and economic method to prepare patterned superhydrophobic membrane and explore their potential as MD membrane. The MD performance of membranes with microscale corrugated surface has not been reported previously. In this communication, a polymeric corrugated substrate (Fig. 1) is used to prepare superhydrophobic polyvinyl fluoride (PVDF) microporous membrane for direct contact membrane distillation (DCMD). Unexpected flux differentiation was, for the first time, observed: MD fluxes are different between a flow parallel to the ridge and a flow perpendicular to the ridge. This anisotropic flux

behavior was correlated to the difference in sliding angles and was possible due to the hydrodynamic disruption at the water-air-solid interface. The results provide a new insight to the potential of hydrophobic micropatterned membranes in membrane distillation.

2. Materials and methods

2.1 Materials and chemicals

The polymer powder, PVDF (Solef 1015) was supplied by Solvay. N, N-Dimethylacetamide (DMAc, AR) and Diethylene glycol (DEG, AR) were provided by Sinopharm Chemical Reagent Co. Ltd. PDMS (Polydimethylsiloxane) and the curing agent (SYLGARD 184) were purchased from Dow Corning Co. Ltd and without further purification before usage. The PEI (polyetherimide) grating template with a corrugated surface was purchased from Suzhou Crystal Silicon Electronic and Technology Co. Ltd. The dimensions of the grating template are showed in Fig. 1.

2.2 Preparation of surface patterned PVDF membranes via μPS

Preparation PDMS mold: Oligomer PDMS and the curing agent (SYLGARD 184, Dow Corning Co. Ltd) were pre-mixed at a weight ratio of 10:1. After de-gassing in vacuum for 10 min, the mixture was cast onto the PEI mold. Then the mold and the PDMS solution was transferred into a vacuum oven and cured for 3 hours at 60 °C. The PDMS replica was then peeled off and stored in a clean container. The entire process was carried out in a clean room.

Preparation of PVDF membrane: Homogeneous PVDF casting solution PVDF/DEG/DMAc (15/27.4/57.6 wt.%) was prepared in a flask at 90°C with vigorous mechanical stirring for 12 h. After filtered using a metal filter of 40 μm, the solution was deaerated at 90 °C. The solution

was then cast on the PDMS mold to a film of 250 μm thickness using a tailor-made stainless-steel casting knife. The PDMS replica was pre-warmed in the oven at 65 °C to avoid any inhomogeneity in temperature during casting. Subsequently, the cast polymer film was exposed to water vapor for 10s (10 cm above coagulation water bath, 75 °C) and immersed in a coagulation bath for 15 minutes to induce precipitation and remove of DEG and DMAc residue. The membrane was further rinsed with water to remove traces of solvent and additives. Before being dried in the oven at 35 °C for 24h, the membrane was rinsed using ethanol. The resultant membrane was coded as patterned corrugated PVDF membrane (C-PVDF). Fig. 1 shows the procedure for the fabrication of patterned PVDF membranes and details are as follows.

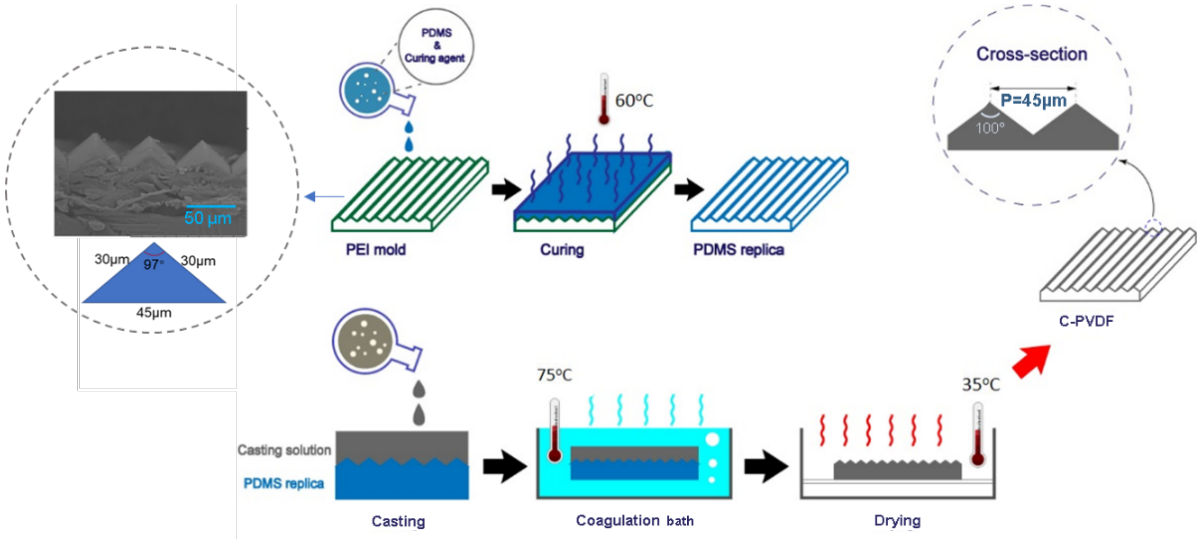

Fig. 1 Schematic for the fabrication of corrugation patterned PVDF membranes (C-PVDF). The patterned PVDF membrane has surface corrugation with the dimension of 45 μm (Period).

2.3 Membrane characterization

The membrane morphology was examined by scanning electron microscopy (SEM) (HITACH TM-1000 and FEI Nova Nano SEM 450). Prior to imaging, membrane samples were coated with a thin layer of gold using a sputter coater. Water contact angle (CA) and sliding

angle (SA) of the membranes were measured using a contact angle goniometer (Maist Drop Meter A-100P) via the sessile drop method. The tilt angle at which the droplet started rolling off the surface was noted as the sliding angle. Pore size was analyzed using porometry (Porolux 1000) [31, 33].

2.4 MD performance

Direct contact MD (DCMD) experiments were performed on a bench-scale membrane test apparatus [23, 34]. Both deionized water and 4 wt.% NaCl solution were tested as the feed and permeate at 60 °C and 20 °C respectively. The patterned side of the C-PVDF membrane was in contact with the feed. Conductivity of the permeate was measured by a conductivity sensor (HQ14d, Hach, CO). The flux (J, kg/m^2·h) was calculated based on Eq. (1):

$$J = \Delta m / A \Delta t. \quad (1)$$

Where Δm (kg) is the amount of water transported from the feed to the permeate, Δt the interval of the collection (h) and A the membrane area (m^2).

3. Results and discussion

3.1 Morphology of the C-PVDF membrane

Fig. 3 shows the SEM images of the top, bottom and cross-section of the C-PVDF membrane. The membrane shows a porous top and bottom surface, as well as a microporous cross-section. The ridges and valleys of the corrugated C-PVDF membranes is characterized as open porous with no visual variations between the ridge and valley (Fig. 2, inserts, magnified). For clarity, the patterned surface facing the feed, is named as the top membrane surface in this work. Fig. 2 shows that the corrugated surface of the C-PVDF membrane (i.e. the top surface) was the one in contact with the PDMS replica during membrane formation.

Upon immersion precipitation, the phase separation started from the top, open surface of the polymer solution (opposite to the PDMS mold); instantaneous demixing occurred at the water/polymer solution interface, resulting in a finger-like macrovoid structure (i.e. C-PVDF cross-section in Fig. 2). However, below this surface, the solvent and additives in the polymer solution close to the PDMS replica had to diffuse across the whole membrane into the water bath, thus allowing enough time for the polymer-lean phases to grow and eventually enlarge into microporous structure [35-38]. The interconnected porous structure in the smooth and corrugated surfaces was resulted from the competition between the solid-liquid phase separation and liquid-liquid separation for a semi-crystalline polymer [39].

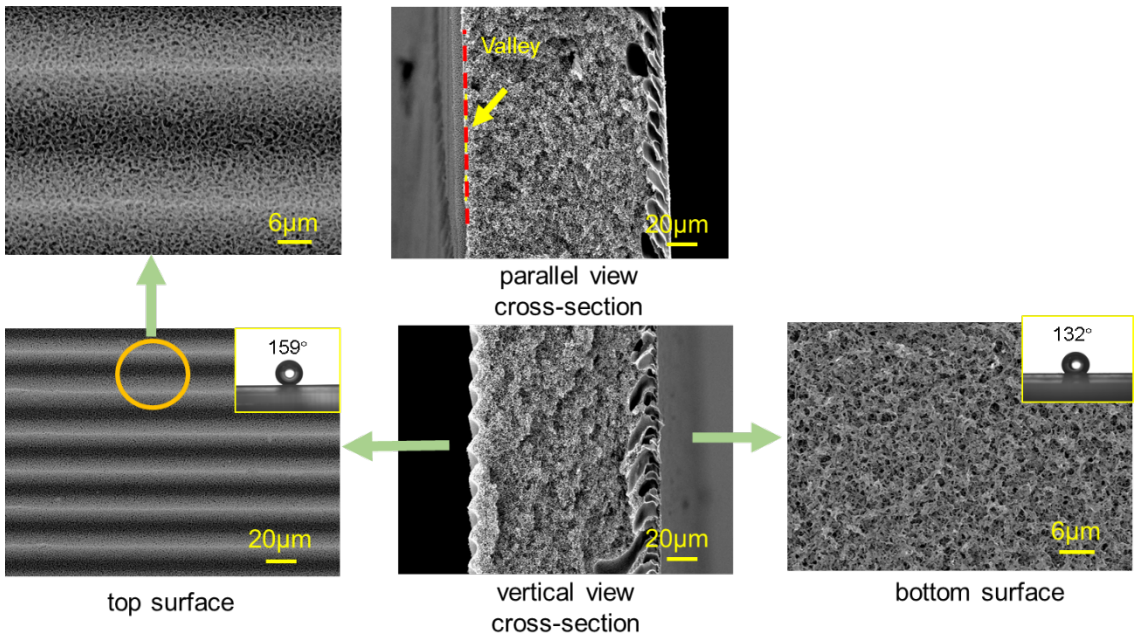

Fig. 2 SEM images of C-PVDF membranes. Notice the parallel view and the vertical view of the cross-section. The top surface in this experiment was the surface facing the feed, but in preparation process, it was in contact with the PDMS mold.

As listed in Table 1, the C-PVDF membrane had a thickness of ~160 μm, and a mean pore size of 0.101 μm. The membrane is relatively thick comparing to the commercial PVDF membranes (of 125 μm) [33]. However, this is adjustable if needed. The membrane is superhydrophobic with a static contact angle of 159 ± 4°. Interestingly, when measuring the sliding angle, a striking difference was found: when the water droplets rolled in parallel with the ridge, a sliding angle of 9.1 ± 0.8° was observed, but a sliding angle of 14.6 ± 1.6° was observed when the water droplets rolled perpendicular to the ridge. To distinguish these two flow modes, we thus define the first as C-PVDF-p and the second mode as C-PVDF-v (using -v instead of –p for clarity). Intuitively, C-PVDF-v mode has slightly higher resistance to the sliding of water droplets than in C-PVDF-p mode. Since the difference in sliding angles are small, no difference would be expected for both orientations. In the following sessions, we will discuss the difference induced by this minor difference on the MD performance.

Table 1. Characteristics of the C-PVDF membrane.

Characteristics	Value
CA of top surface (°)	159 ± 4
CA of bottom surface (°)	132 ± 3
Mean pore size (μm)	0.101 ± 0.010
Thickness (μm)	160 ± 5
Sliding angle-p (°)	9.1 ± 0.8
Sliding angle-v (°)	14.6 ± 1.6

170 3.2 MD performance

171 The DCMD fluxes with both parallel (C-PVDF-p) and perpendicular (C-PVDF-v) modes
172 are shown in Fig. 3a using deionized water as feed. In 120 min, an obviously higher constant
173 flux of 26.6 kg/m^2·h was observed in the C-PVDF-p mode than in the C-PVDF-v mode (21.6
174 kg/m^2·h). This means that when water flows in parallel to the ridge, there is an increase of
175 about 25% in flux compared to the case when water flows perpendicular to the ridge. To
176 confirm this observation, a simulated seawater containing 40 g/L NaCl as the feed (Fig. 3b)
177 was tested; again, the flux of the C-PVDF-p mode was found about 10% higher than that of the
178 C-PVDF-v mode. No obvious flux decrease was observed for both C-PVDF-p and C-PVDF-v
179 membranes in a test for 60 minutes due to nearly constant salt concentration in the feed.

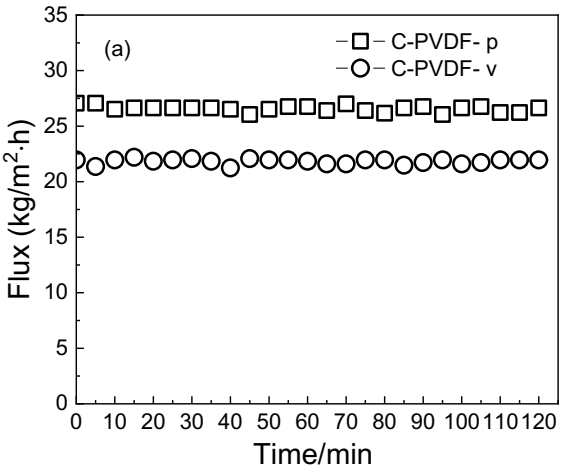

180

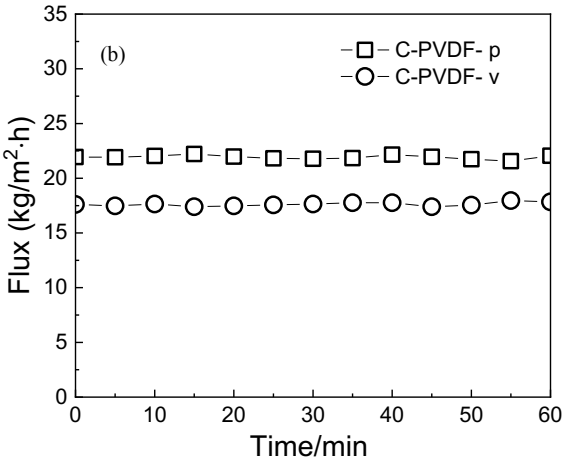

Fig. 3 Effect of the flow directions in relation to the corrugation pattern on DCMD Fluxes of C-PVDF membranes. C-PVDF-p represents feed flow in parallel to the ridge; C-PVDF-p represents feed flow in perpendicular to the ridge. (a) feed: deionized water; (b) 40 g/L NaCl solution. Feed temperature: 60.0±1.0 ^{o}C; permeate temperature: 20.0±1.0 ^{o}C. Flow rate of both feed and permeate: 600 ml/min. Rejection of the membrane for NaCl was 100% using 40 g/L NaCl solution as the feed.

3.3 Analysis for the origin of anisotropy flux

In average, the flow direction to the orientation of the ridge in principal does not affect the mass transfer in MD, thus the flux. According to the Gas-Dusty model [40] , the MD flux is linearly correlated to the water vapor pressure difference across the membrane and the membrane material and morphology, but not directly related to the flow direction. Because of the membrane was exactly the same, thermal conductivity is also not directly related to the flow direction. Theoretically, the flux should be independent from the flow, either in parallel or perpendicular to the ridge. However, the experimental results do not obey the conventional Gas-Dusty model.

Previous studies showed that a superhydrophobic membrane had an increased MD flux in

198 comparison to the pristine one with similar morphology [20, 41] [42]. The observed high MD
199 flux was understood by taking into account of enlarged evaporation surface area in the
200 superhydrophobic PVDF membranes [20, 41]. However, for the corrugated surface studied in
201 this work, the same static contact angles were observed regardless of the flow direction (Table
202 1). Thus, previous theory on the enlarged evaporation area was not applicable from the point
203 view of the static contact angle as two directions would show the same evaporation area.
204 However, evaporation area was still one of the important key factors in determining MD flux
205 [17].

206 Anisotropic wetting of patterned surfaces has been discovered in previous researchers [43-
207 45], however mainly on a dense surface structure, not on a porous surface structure as reported
208 in this paper. Within similar dimensions, the wetting anisotropy ($\Delta\theta$) is strongly related to the
209 groove height, but not greatly depended on period and width [46]. Fig. 4 shows that the wetting
210 anisotropy ($\Delta\theta$) of our C-PVDF membrane is about 10^{o}. with great angle at the parallel view.
211 This anisotropic phenomenon is similar to literature reported results, but to a significantly
212 lesser extent [43-45]. This may be related to the polymer materials we used in this experiment,
213 PVDF, and the surface porosity in the membrane.

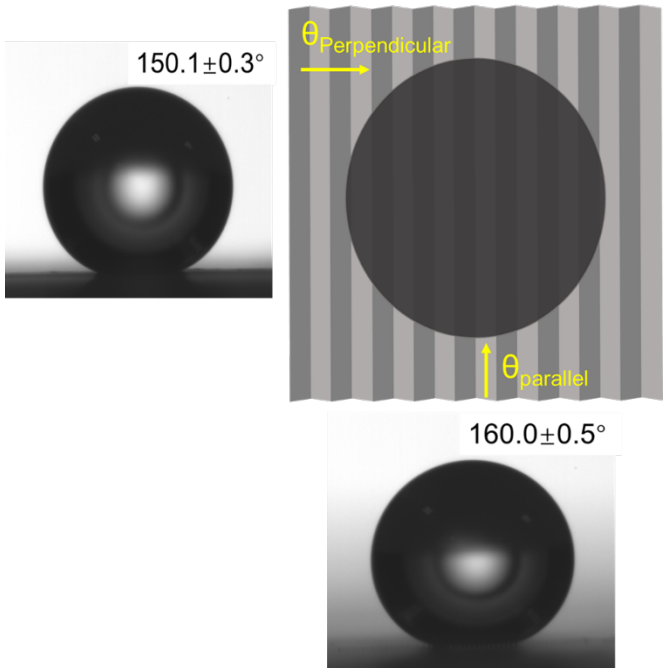

Fig. 4 Images of water droplets on corrugated PVDF membrane surface showing slight anisotropic wetting at parallel and perpendicular directions (Top right hand picture only for schematic demonstration). Note that the view point for measurement is the same as those in flow. The water contact angle measured from parallel view is slightly larger than greater than that measured from the perpendicular view.

Because high energy is required for surpassing the energy barrier created by anisotropic geometry, the contact angle is raised for movement of the contact lines [43]. This results in a higher contact angle at the parallel view, but a lower angle at the perpendicular view. The other anisotropy is demonstrated in the sliding angles as listed in Table 1. Much lower sliding angle was observed at parallel direction, corresponding to the greater water contact angle at the parallel view. There seems a strong correlation between the thermodynamic measurement (contact angle) and dynamics measurement (sliding angle). By evaluating the sliding angle, a simple calculation shows that the drag force in parallel to the ridge is about 0.62 (< 2/3) of that

in perpendicular direction (the ratio of the drag force in two directions = Sin (9.1°)/Sin (14.6°) = 0.62). Intuitively, a small difference of a few degrees in the sliding angle means a small difference in the drag force, but in reality, water droplets encounter much less drag force in the parallel direction (about 38%) than in the perpendicular direction. This direct us to a hypothesis for the flux differentiation at two directions with a hydrodynamic interfacial origin. A quantitative correlation is possible if direct observation of the interface is realized. Since this experimental observation is out of scope of the conventional static view on the hydrophobic membrane surface, a new hydrodynamic analysis will add a new dimension to a more comprehensive understanding of the interface in membrane distillation.

The finding of anisotropic performance for MD membranes with corrugated pattern is unexpected, but intriguing. Scientific understand of such phenomenon is important for future design of patterned surfaces for high performance. Increase in the flux would result in reduced membrane surface area, small footprint as well as capital investment. The fouling/scaling behavior of surface patterned membrane might also be improved at optimized ridge height/period/angle for corrugated surface.

4. Conclusions

Superhydrophobic polyvinylidene fluoride (PVDF) membranes with well-controlled corrugated pattern were prepared via a micromolding phase separation technology. The membrane showed a high static contact angle of 159 ± 4 and an average pore size of 0.1 μm. Surprising anisotropic MD flux was observed when the feed flows in a parallel and perpendicular orientation to the ridge of the pattern. For both deionized water and NaCl

solution, obviously higher flux was found in parallel orientation. This deviation cannot be explained by the Dusty-Gas model because the average characteristics of the membrane in the model are intrinsically the same for both flow modes. Instead, anisotropic wetting and sliding in the parallel and perpendicular orientation revealed both thermodynamic and hydrodynamic origins of our new findings. The present observation has revealed the limitation of the conventional MD model in analysis of micro-patterned surperhydrophobic surface.

Acknowledgements

The research was partially supported by National Natural Science Foundation of China (No. 21978315, 21676290, 51861145313, 21808236), and Newton Advanced Fellowship (Grant No. NA170113).

References

[1] A. Alkhudhiri, N. Darwish, N. Hilal, Membrane distillation: A comprehensive review, Desalination, 287 (2012) 2-18.

[2] L.D. Tijing, Y.C. Woo, J.-S. Choi, S. Lee, S.-H. Kim, H.K. Shon, Fouling and its control in membrane distillation—A review, Journal of Membrane Science, 475 (2015) 215-244.

[3] A. Deshmukh, C. Boo, V. Karanikola, S. Lin, M. Elimelech, Membrane Distillation at the Water-Energy Nexus: Limits, Opportunities, and Challenges, Energy & Environmental Science, 11 (2018) 10.1039.C1038EE00291F.

[4] D.M. Warsinger, J. Swaminathan, E. Guillen-Burrieza, H.A. Arafat, J.H. Lienhard V, Scaling and fouling in membrane distillation for desalination applications: A review,

Desalination, 356 (2015) 294-313.

[5] J. Choi, Y. Choi, Y. Jang, Y. Shin, S. Lee, Effect of aeration on CaSO4 scaling in membrane distillation process, Desalination and Water Treatment, 90 (2017) 7-15.

[6] G. Naidu, S. Jeong, S. Vigneswaran, Influence of feed/permeate velocity on scaling development in a direct contact membrane distillation, Separation and Purification Technology, 125 (2014) 291-300.

[7] M. Gryta, Polyphosphates used for membrane scaling inhibition during water desalination by membrane distillation, Desalination, 285 (2012) 170-176.

[8] M. Gryta, K. Karakulski, M. Tomaszewska, A. Morawski, Treatment of effluents from the regeneration of ion exchangers using the MD process, Desalination, 180 (2005) 173-180.

[9] C. Boo, J. Lee, M. Elimelech, Engineering Surface Energy and Nanostructure of Microporous Films for Expanded Membrane Distillation Applications, Environmental Science & Technology, 50 (2016) 8112-8119.

[10] A. Razmjou, E. Arifin, G. Dong, J. Mansouri, V. Chen, Superhydrophobic modification of TiO2 nanocomposite PVDF membranes for applications in membrane distillation, Journal of Membrane Science, 415 (2012) 850-863.

[11] S. Lin, S. Nejati, C. Boo, Y. Hu, C.O. Osuji, M. Elimelech, Omniphobic Membrane for Robust Membrane Distillation, Environmental Science & Technology Letters, 1 (2014) 443-447.

[12] L.H. Chen, A. Huang, Y.R. Chen, C.H. Chen, C.C. Hsu, F.Y. Tsai, K.L. Tung, Omniphobic membranes for direct contact membrane distillation: Effective deposition of zinc oxide nanoparticles, Desalination, 428 (2018) 255-263.

[13] Z. Xiao, R. Zheng, Y. Liu, H. He, X. Yuan, Y. Ji, D. Li, H. Yin, Y. Zhang, X.-M. Li, T. He, Slippery for scaling resistance in membrane distillation: A novel porous micropillared superhydrophobic surface, Water Research, 155 (2019) 152-161.

[14] M. Xie, W. Luo, S.R. Gray, Surface pattern by nanoimprint for membrane fouling mitigation: Design, performance and mechanisms, Water Research, 124 (2017) 238-243.

[15] C. Boo, J. Lee, M. Elimelech, Omniphobic Polyvinylidene Fluoride (PVDF) Membrane for Desalination of Shale Gas Produced Water by Membrane Distillation, Environ Sci Technol, 50 (2016) 12275-12282.

[16] J. Lee, C. Boo, W.H. Ryu, A.D. Taylor, M. Elimelech, Development of Omniphobic Desalination Membranes Using a Charged Electrospun Nanofiber Scaffold, ACS Appl Mater Interfaces, 8 (2016) 11154-11161.

[17] W. Wang, X. Du, H. Vahabi, S. Zhao, Y. Yin, A.K. Kota, T. Tong, Trade-off in membrane distillation with monolithic omniphobic membranes, Nature Communications, 10 (2019).

[18] M. Tian, Y. Yin, C. Yang, B. Zhao, J. Song, J. Liu, X.-M. Li, T. He, CF4 plasma modified highly interconnective porous polysulfone membranes for direct contact membrane distillation (DCMD), Desalination, 369 (2015) 105-114.

[19] X. Wei, B. Zhao, X.-M. Li, Z. Wang, B.-Q. He, T. He, B. Jiang, CF4 plasma surface modification of asymmetric hydrophilic polyethersulfone membranes for direct contact membrane distillation, Journal of Membrane Science, 407-408 (2012) 164-175.

[20] C. Yang, X.-M. Li, J. Gilron, D.-f. Kong, Y. Yin, Y. Oren, C. Linder, T. He, CF4 plasma-modified superhydrophobic PVDF membranes for direct contact membrane distillation, Journal of Membrane Science, 456 (2014) 155-161.

[21] Y. Chen, M. Tian, X. Li, Y. Wang, A.K. An, J. Fang, T. He, Anti-wetting behavior of negatively charged superhydrophobic PVDF membranes in direct contact membrane distillation of emulsified wastewaters, Journal of membrane science, 535 (2017) 230-238.

[22] Y.C. Woo, Y. Chen, L.D. Tijing, S. Phuntsho, T. He, J.-S. Choi, S.-H. Kim, H.K. Shon, CF4 plasma-modified omniphobic electrospun nanofiber membrane for produced water brine treatment by membrane distillation, Journal of Membrane Science, 529 (2017) 234-242.

[23] R. Zheng, Y. Chen, J. Wang, J. Song, X.-M. Li, T. He, Preparation of omniphobic PVDF membrane with hierarchical structure for treating saline oily wastewater using direct contact membrane distillation, Journal of membrane science, 555 (2018) 197-205.

[24] O. Heinz, M. Aghajani, A.R. Greenberg, Y. Ding, Surface-patterning of polymeric membranes: fabrication and performance, Current Opinion in Chemical Engineering, 20 (2018) 1-12.

[25] S.H. Maruf, A.R. Greenberg, Y. Ding, Influence of substrate processing and interfacial polymerization conditions on the surface topography and permselective properties of surface-patterned thin-film composite membranes, Journal of Membrane Science, 512 (2016) 50-60.

[26] P.Z. Çulfaz, M. Wessling, R.G.H. Lammertink, Hollow fiber ultrafiltration membranes with microstructured inner skin, Journal of Membrane Science, 369 (2011) 221-227.

[27] A.M. Peters, R.G.H. Lammertink, M. Wessling, Comparing flat and micro-patterned surfaces: Gas permeation and tensile stress measurements, Journal of Membrane Science, 320 (2008) 173-178.

[28] S.Y. Jung, Y.-J. Won, J.H. Jang, J.H. Yoo, K.H. Ahn, C.-H. Lee, Particle deposition on the patterned membrane surface: Simulation and experiments, Desalination, 370 (2015) 17-24.

[29] Y.-J. Won, S.-Y. Jung, J.-H. Jang, J.-W. Lee, H.-R. Chae, D.-C. Choi, K.H. Ahn, C.-H. Lee, P.-K. Park, Correlation of membrane fouling with topography of patterned membranes for water treatment, Journal of membrane science, 498 (2016) 14-19.

[30] J.A. Kharraz, M.R. Bilad, H.A. Arafat, Flux stabilization in membrane distillation desalination of seawater and brine using corrugated PVDF membranes, Journal of Membrane Science, 495 (2015) 404-414.

[31] Z. Xiao, Z. Li, H. Guo, Y. Liu, Y. Wang, H. Yin, X. Li, J. Song, L.D. Nghiem, T. He, Scaling mitigation in membrane distillation: From superhydrophobic to slippery, Desalination, 466 (2019) 36-43.

[32] Z. Xiao, G. Hong, H. He, Y. Liu, X. Li, Y. Zhang, H. Yin, T. He, Unprecedented scaling/fouling resistance of omniphobic polyvinylidene fluoride membrane with silica nanoparticle coated micropillars in direct contact membrane distillation, Journal of Membrane Science, 599 (2020) 117819.

[33] J. Wang, H. He, M. Wang, Z. Xiao, Y. Chen, Y. Wang, J. Song, X.-M. Li, Y. Zhang, T. He, 3-[[3-(Triethoxysilyl)-propyl] amino] propane-1-sulfonic acid zwitterion grafted polyvinylidene fluoride antifouling membranes for concentrating greywater in direct contact membrane distillation, Desalination, 455 (2019) 71-78.

[34] Y. Chen, R. Zheng, J. Wang, Y. Liu, Y. Wang, X.-M. Li, T. He, Laminated PTFE membranes to enhance the performance in direct contact membrane distillation for high salinity solution, Desalination, 424 (2017) 140-148.

[35] X.-M. Li, Y. Ji, Y. Yin, Y.-Y. Zhang, Y. Wang, T. He, Origin of delamination/adhesion in polyetherimide/polysulfone co-cast membranes, Journal of Membrane Science, 352 (2010)

358 173-179.
359 [36] Y. Ji, X.-M. Li, Y. Yin, Y.-Y. Zhang, Z.-W. Wang, T. He, Morphological control and cross-
360 flow filtration of microfiltration membranes prepared via a sacrificial-layer approach, Journal
361 of Membrane Science, 353 (2010) 159-168.
362 [37] X.M. Li, Y. Ji, T. He, M. Wessling, A sacrificial-layer approach to prepare microfiltration
363 membranes, Journal of Membrane Science, 320 (2008) 1-7.
364 [38] T. He, M.H.V. Mulder, M. Wessling, Preparation of porous hollow fiber membranes with
365 a triple-orifice spinneret, Journal of Applied Polymer Science, 87 (2003) 2151-2157.
366 [39] L. Xing, J. Song, Z. Li, J. Liu, T. Huang, P. Dou, Y. Chen, X.-M. Li, T. He, Solvent stable
367 nanoporous poly (ethylene-co-vinyl alcohol) barrier membranes for liquid-liquid extraction of
368 lithium from a salt lake brine, Journal of Membrane Science, 520 (2016) 596-606.
369 [40] R.W. Schofield, A.G. Fane, C.J.D. Fell, Heat and mass transfer in membrane distillation,
370 Journal of Membrane Science, 33 (1987) 299-313.
371 [41] C. Yang, M. Tian, Y. Xie, X.-M. Li, B. Zhao, T. He, J. Liu, Effective evaporation of CF4
372 plasma modified PVDF membranes in direct contact membrane distillation, Journal of
373 Membrane Science, 482 (2015) 25-32.
374 [42] E.-J. Lee, A.K. An, T. He, Y.C. Woo, H.K. Shon, Electrospun nanofiber membranes
375 incorporating fluorosilane-coated TiO2 nanocomposite for direct contact membrane distillation,
376 Journal of Membrane Science, 520 (2016) 145-154.
377 [43] J.Y. Chung, J.P. Youngblood, C.M. Stafford, Anisotropic wetting on tunable micro-
378 wrinkled surfaces, Soft Matter, 3 (2007) 1163.
379 [44] M. Morita, T. Koga, H. Otsuka, A. Takahara, Macroscopic-Wetting Anisotropy on the

380 Line-Patterned Surface of Fluoroalkylsilane Monolayers, Langmuir 21 (2005) 911-918.
381 [45] Y. Ding, J. Sun, H.W. Ro, Z. Wang, J. Zhou, N.J. Lin, M.T. Cicerone, C.L. Soles, S. Lin-
382 Gibson, Thermodynamic underpinnings of cell alignment on controlled topographies,
383 Advanced materials, 23 (2011) 421-425.
384 [46] D. Xia, L.M. Johnson, G.P. Lopez, Anisotropic wetting surfaces with one-dimensional and
385 directional structures: fabrication approaches, wetting properties and potential applications,
386 Advanced materials, 24 (2012) 1287-1302.
387